

CERN-TH/97-324
hep-ph/9711407
November 1997

MSSM Higgs Boson Production at the LHC ^{*}

Michael Spira

CERN, Theory Division, CH-1211 Geneva 23, Switzerland

Abstract

The theoretical status of Higgs boson production at the LHC within the minimal supersymmetric extension of the Standard Model is reviewed. The focus will be on the evaluation of higher-order corrections to the production cross sections and their phenomenological implications.

CERN-TH/97-324
hep-ph/9711407
November 1997

^{*}Contribution to the proceedings of the *International Workshop on Quantum Effects in the MSSM*, 9–13 September 1997, Barcelona, Spain

MSSM Higgs Boson Production at the LHC

MICHAEL SPIRA

CERN, Theory Division, CH-1211 Geneva 23, Switzerland

E-mail: Michael.Spira@cern.ch

The theoretical status of Higgs boson production at the LHC within the minimal supersymmetric extension of the Standard Model is reviewed. The focus will be on the evaluation of higher-order corrections to the production cross sections and their phenomenological implications.

1 Introduction

The search for Higgs bosons is one of the most important goals for present and future experiments. Once a Higgs will be found, its properties have to be investigated in order to distinguish between the Standard Model [SM] and its extensions. Supersymmetry represents one of the most attractive extensions, since it provides a natural solution to the hierarchy problem of the SM. The minimal supersymmetric extension of the SM [MSSM] contains two isospin doublets of Higgs fields, which are necessary to allow to introduce up and down-quark masses without breaking supersymmetry¹. Moreover, they are required to cancel anomalies associated with Higgsinos, the supersymmetric partners of the Higgs bosons. After electroweak symmetry breaking, one is left with a spectrum of 5 elementary Higgs particles: two neutral CP-even (h, H), one neutral CP-odd (A) and two charged (H^\pm) Higgs bosons. The MSSM Higgs sector can be described by two independent parameters at leading order (LO), which are in general chosen as $\text{tg}\beta = v_2/v_1$, i.e. the ratio of the two vacuum expectation values of the scalar Higgs fields, and the pseudoscalar mass M_A . Radiative corrections to the Higgs masses and couplings are large², since the leading part ϵ grows as the fourth power of the top-quark mass m_t :

$$\epsilon = \frac{3G_F}{\sqrt{2}\pi^2} \frac{m_t^4}{\sin^2\beta} \log \left(1 + \frac{\tilde{m}_s^2}{m_t^2} \right) \quad (1)$$

where G_F denotes the Fermi constant and \tilde{m}_s the common squark mass. They shift the upper bound on the light scalar Higgs mass to $M_h \lesssim 130$ GeV. The Higgs couplings to top (bottom) quarks and gauge bosons are modified by SUSY factors, which are collected in Table 1. The angle α denotes the mixing angle between the scalar Higgs particles h, H . An important property of the SUSY couplings is the enhancement (suppression) of the bottom (top) Yukawa coupling for increasing $\text{tg}\beta$. The direct search for the MSSM Higgs particles

at LEP yields lower limits $M_{h,H,A} \gtrsim 62.5$ GeV for the neutral Higgs masses³.

Table 1: *Higgs couplings in the MSSM to fermions and gauge bosons [V = W, Z] relative to SM couplings.*

ϕ		g_t^ϕ	g_b^ϕ	g_V^ϕ
SM	H	1	1	1
MSSM	h	$\cos \alpha / \sin \beta$	$-\sin \alpha / \cos \beta$	$\sin(\beta - \alpha)$
	H	$\sin \alpha / \sin \beta$	$\cos \alpha / \cos \beta$	$\cos(\beta - \alpha)$
	A	$1/\tan \beta$	$\tan \beta$	0

At the LHC, the production of neutral Higgs bosons[†] is dominated by gluon fusion $gg \rightarrow \phi$ [$\phi = h, H, A$]⁴. Only for large values of $\tan \beta$ does Higgs bremsstrahlung off bottom quarks, $gg, q\bar{q} \rightarrow \phi b\bar{b}$, become dominant. This is shown in Fig. 1, in which the Higgs boson production cross sections via the various mechanisms for the scalar and pseudoscalar Higgs particles at the LHC are presented. For their discovery, several decay modes must be exploited in different regions of the MSSM parameter space⁸: $h \rightarrow \gamma\gamma$; $H, A \rightarrow \tau^+\tau^-$; $H \rightarrow hh \rightarrow b\bar{b}\gamma\gamma$; $A \rightarrow ZH \rightarrow \ell^+\ell^-b\bar{b}$; $H, A \rightarrow t\bar{t}$.

2 $gg \rightarrow \phi$

2.1 Lowest order

At LO the gluon fusion mechanism is mediated by heavy top, bottom and squark loops, see Fig. 2. The LO cross sections are given by^{4,9}

$$\sigma_{LO}(pp \rightarrow \phi) = \sigma_0^\phi \tau_\phi \frac{d\mathcal{L}^{gg}}{d\tau_\phi} \quad (2)$$

$$\sigma_0^{h/H} = \frac{G_F \alpha_s^2(\mu)}{288\sqrt{2}\pi} \left| \sum_Q g_Q^{h/H} A_Q^{h/H}(\tau_Q) + \sum_{\tilde{Q}} g_{\tilde{Q}}^{h/H} A_{\tilde{Q}}^{h/H}(\tau_{\tilde{Q}}) \right|^2$$

$$\sigma_0^A = \frac{G_F \alpha_s^2(\mu)}{128\sqrt{2}\pi} \left| \sum_Q g_Q^A A_Q^A(\tau_Q) \right|^2$$

[†]Charged Higgs bosons will be produced via radiation from a top quark⁵ or in pairs via the Drell-Yan process⁶ or gluon-gluon collisions⁷. They will not be considered here.

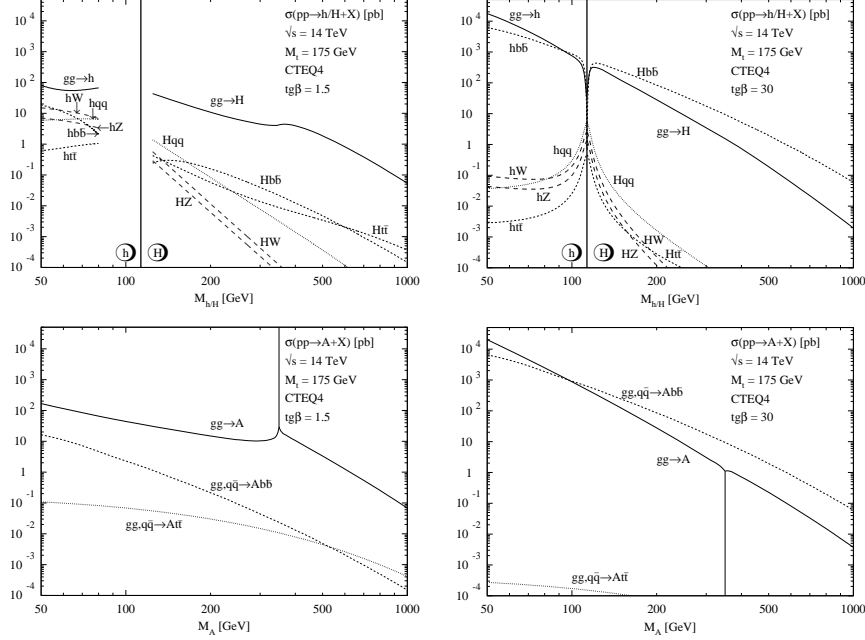


Figure 1: Neutral MSSM Higgs production cross sections at the LHC [$\sqrt{s} = 14$ TeV] for gluon fusion $gg \rightarrow \phi$, vector-boson fusion $qq \rightarrow qqVV \rightarrow qqh/qqH$, vector-boson bremsstrahlung $q\bar{q} \rightarrow V^* \rightarrow hV/HV$ and the associated production $gg, q\bar{q} \rightarrow \phi b\bar{b}/\phi t\bar{t}$ including all known QCD corrections for $\text{tg}\beta = 1.5, 30$.

with the scaling variables $\tau_\phi = M_\phi^2/s$ and $\tau_{Q,\tilde{Q}} = 4m_{Q,\tilde{Q}}^2/M_\phi^2$ and the function

$$f(\tau) = \begin{cases} \arcsin^2 \frac{1}{\sqrt{\tau}} & \tau \geq 1 \\ -\frac{1}{4} \left[\log \frac{1 + \sqrt{1 - \tau}}{1 - \sqrt{1 - \tau}} - i\pi \right]^2 & \tau < 1 \end{cases} \quad (3)$$

\mathcal{L}^{gg} denotes the gluon luminosity. The top and bottom quarks as well as the third-generation squarks provide the dominant contributions to the cross sections. Because of the behavior of the SUSY couplings the top (bottom) contributions are suppressed (enhanced) for large $\text{tg}\beta$. The squark contributions are sizeable only if the squark mass is below ~ 400 GeV, as can be seen in Fig. 3, where the ratio of the light scalar Higgs production cross sections with and without the squark loops is shown as a function of the squark mass^{10,11}.

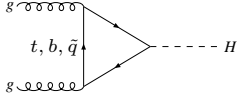


Figure 2: Diagrams contributing to $gg \rightarrow H$ at lowest order.

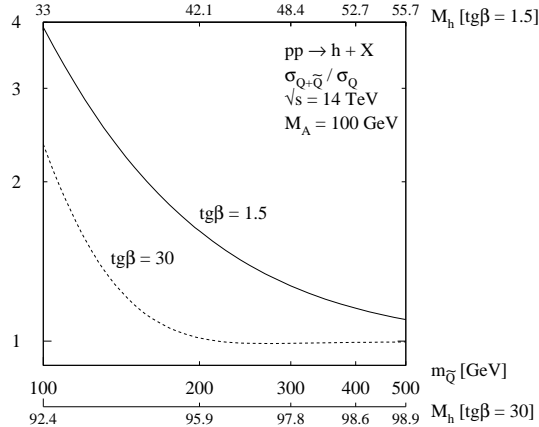


Figure 3: Ratio of the cross section $\sigma(pp \rightarrow h + X)$ with and without squark loops as a function of the common squark mass $m_{\tilde{Q}}$ for two values of $\tan\beta = 1.5, 30$, and for $M_A = 100$ GeV. The secondary axes present the corresponding light scalar Higgs mass M_h .

2.2 QCD corrections

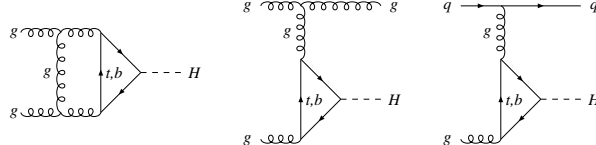


Figure 4: Typical diagrams contributing to the virtual and real QCD corrections to $gg \rightarrow H$.

Quark loops. The NLO QCD corrections consist of two-loop virtual corrections and one-loop real corrections from the processes $gg \rightarrow Hg, gg \rightarrow Hq, q\bar{q} \rightarrow Hg$. Typical diagrams are depicted in Fig. 4. The evaluation of the virtual and real corrections has been performed within dimensional regularization. The five-dimensional Feynman integrals of the two-loop diagrams have been reduced analytically to one-dimensional ones, which have been integrated numerically. The tensor reduction of the virtual three-point functions cannot be performed completely down to scalar integrals, but one is left with the calculation of irreducible tensor integrals. The heavy quark mass has been

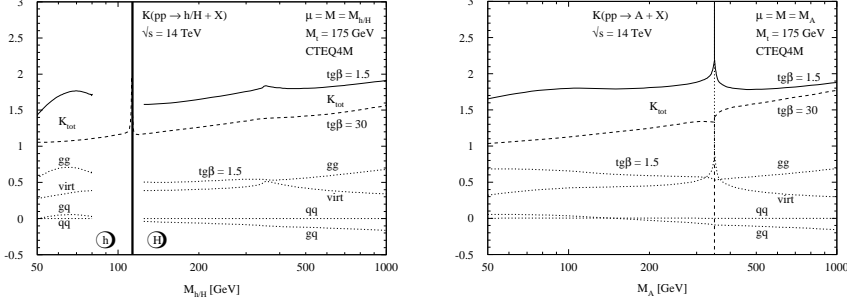


Figure 5: K factors of the QCD-corrected gluon-fusion cross section $\sigma(pp \rightarrow \phi + X)$ at the LHC with c.m. energy $\sqrt{s} = 14$ TeV. The dashed lines show the individual contributions of the four terms of the QCD corrections given in eq. (4). The renormalization and factorization scales have been identified with the corresponding Higgs mass, $\mu = M = M_\phi$, and the CTEQ4M parton densities have been adopted.

renormalized on-shell and the strong coupling α_s in the $\overline{\text{MS}}$ scheme. The remaining collinear singularities of the real corrections are absorbed in the NLO parton densities, defined in the $\overline{\text{MS}}$ scheme. In order to calculate the QCD corrections to the pseudoscalar Higgs boson production, a consistent scheme for the γ_5 coupling has to be used. We implemented the 't Hooft–Veltman scheme¹², its modification by Larin¹³ and the scheme introduced by Kreimer¹⁴, all schemes giving identical results; for a naive γ_5 the final result turned out to be ambiguous and thus inconsistent, as a result of the ABJ anomaly¹⁷. The cross sections can be cast into the form⁹

$$\begin{aligned} \sigma(pp \rightarrow \phi + X) &= \sigma_0^\phi \left[1 + C^\phi \frac{\alpha_s}{\pi} \right] \tau_\phi \frac{d\mathcal{L}^{gg}}{d\tau_\phi} + \Delta\sigma_{gg}^\phi + \Delta\sigma_{gq}^\phi + \Delta\sigma_{qq}^\phi \quad (4) \\ C^\phi(\tau_Q) &= \pi^2 + c^\phi(\tau_Q) + \frac{33 - 2N_F}{6} \log \frac{\mu^2}{M_\phi^2} \\ \Delta\sigma_{gg}^\phi &= \int_{\tau_\phi}^1 d\tau \frac{d\mathcal{L}^{gg}}{d\tau} \times \frac{\alpha_s}{\pi} \sigma_0^\phi \left\{ -z P_{gg}(z) \log \frac{M^2}{\hat{s}} + d_{gg}^\phi(z, \tau_Q) \right. \\ &\quad \left. + 12 \left[\left(\frac{\log(1-z)}{1-z} \right)_+ - z[2-z(1-z)] \log(1-z) \right] \right\} \\ \Delta\sigma_{gq}^\phi &= \int_{\tau_\phi}^1 d\tau \sum_{q,\bar{q}} \frac{d\mathcal{L}^{gq}}{d\tau} \times \frac{\alpha_s}{\pi} \sigma_0^\phi \left\{ -\frac{z}{2} P_{gq}(z) \log \frac{M^2}{\hat{s}(1-z)^2} \right. \\ &\quad \left. + d_{gq}^\phi(z, \tau_Q) \right\} \end{aligned}$$

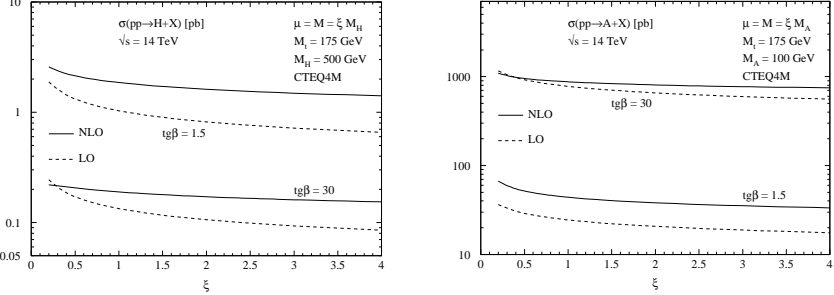


Figure 6: The renormalization and factorization scale dependence of the Higgs production cross section at lowest and next-to-leading order for two different Higgs bosons H, A with masses $M_H = 500$ GeV and $M_A = 100$ GeV and two values of $\text{tg}\beta = 1.5, 30$.

$$\Delta\sigma_{q\bar{q}}^\phi = \int_{\tau_\phi}^1 d\tau \sum_q \frac{d\mathcal{L}^{q\bar{q}}}{d\tau} \times \frac{\alpha_s}{\pi} \sigma_0^\phi d_{q\bar{q}}^\phi(z, \tau_Q)$$

with $z = \tau_\phi/\tau = M_\phi^2/\hat{s}$. P_{gg} and P_{gq} are the standard Altarelli–Parisi splitting functions¹⁵. The K factors $K = \sigma_{NLO}/\sigma_{LO}$, where the NLO (LO) cross sections have been evaluated with NLO (LO) α_s and parton densities, are presented in Fig. 5 as functions of the corresponding Higgs masses. The QCD corrections are large and positive, increasing the production cross sections by 10–100%⁹, so that they can no longer be neglected. In spite of the large size of the QCD corrections the scale dependence is reduced significantly, rendering these NLO results reliable within $\sim 20\%$ ⁹, as can be seen in Fig. 6, which shows the LO and NLO cross sections as a function of the common renormalization and factorization scales in units of the corresponding Higgs masses. Improved measurements of the parton densities in the HERA experiments reduced the uncertainties from the parton densities to a level of $\sim 15\%$ ⁹. The size of the K factors depends strongly on $\text{tg}\beta$ ⁹.

In the limit of heavy quark masses the mass-dependent terms of Eq. 4 reduce to very simple expressions⁹:

$$\begin{aligned} c^{h,H}(\tau_Q) &\rightarrow \frac{11}{2} & c^A(\tau_Q) &\rightarrow 6 & d_{gg}(z, \tau_Q) &\rightarrow -\frac{11}{2}(1-z)^3 \\ d_{gq}(z, \tau_Q) &\rightarrow \frac{2}{3}z^2 - (1-z)^2 & d_{q\bar{q}}(z, \tau_Q) &\rightarrow \frac{32}{27}(1-z)^3 \end{aligned} \quad (5)$$

These limits can also be derived from low-energy theorems.

Low-energy theorems. For scalar Higgs bosons these rely on the fact that for vanishing Higgs momentum the entire interaction of the Higgs particle with

fermions and gauge bosons can be generated by a shift of masses by the Higgs field. Thus matrix elements with an external light Higgs boson are related to the matrix element without the Higgs boson¹⁶:

$$\lim_{p_H \rightarrow 0} \mathcal{M}_0(XH) = \frac{g^\phi}{v_0} m_0 \frac{\partial}{\partial m_0} \mathcal{M}_0(X) \quad (6)$$

where X denotes any particle configuration, $v = 1/\sqrt{\sqrt{2}G_F}$ the vacuum expectation value, and g^ϕ the corresponding SUSY coupling of Table 1. In order to extend this relation to higher orders in perturbation theory, it must be formulated in terms of bare quantities⁹. For on-shell Higgs particles this mathematical limit coincides with the massless Higgs limit. Thus we can derive the effective coupling of a light Higgs boson to gluons from the gluon self-energy⁹,

$$\mathcal{L}_{eff} = \frac{\alpha_s}{12\pi} G^{a\mu\nu} G_{\mu\nu}^a \frac{H}{v} \left\{ 1 + \frac{11\alpha_s}{4\pi} + \mathcal{O}(\alpha_s^2) \right\} \quad (7)$$

This Lagrangian has to be interpreted as part of the basic Lagrangian describing the effective theory, once the top quark is integrated out, and thus provides the proper description of the heavy quark limit. The effective coupling has to be inserted in the blobs of the effective diagrams shown in Fig. 7. The final result coincides with Eqs. 4,5 of the scalar Higgs bosons.

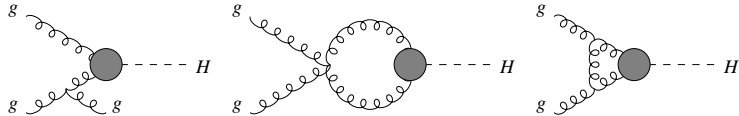


Figure 7: Typical effective diagrams contributing to the QCD corrections to $gg \rightarrow H$.

The low-energy theorems for pseudoscalar Higgs particles are based on the ABJ anomaly in the divergence of the axial-vector current¹⁷,

$$\partial^\mu j_\mu^5 = 2m_Q \bar{Q} i\gamma_5 Q + \frac{\alpha_s}{2\pi} G^{a\mu\nu} \tilde{G}_{\mu\nu}^a \quad (8)$$

with $\tilde{G}_{\mu\nu}^a = \frac{1}{2}\epsilon_{\mu\nu\alpha\beta}G^{a\alpha\beta}$ denoting the dual field strength tensor. The axial-vector current operator fulfills the low-energy condition¹⁸

$$\langle gg | \partial_\mu j_5^\mu A | A \rangle \rightarrow 0 \quad \text{for } p_A \rightarrow 0 \quad (9)$$

Using the basic interaction $\mathcal{L}_{int} = -g_Q^A m_Q \bar{Q} i\gamma_5 Q A/v$ the effective Lagrangian for the Agg coupling can be derived⁹:

$$\mathcal{L}_{eff} = g_Q^A \frac{\alpha_s}{4\pi} G^{a\mu\nu} \tilde{G}_{\mu\nu}^a \frac{A}{v} \quad (10)$$

Due to the Adler–Bardeen theorem of the non-renormalization of the ABJ anomaly¹⁹, this effective Lagrangian is valid up to all orders of perturbation theory. Its insertion into the effective diagrams analogous to Fig. 7 leads to the results of Eqs. 4.5 of the pseudoscalar Higgs boson.

Squark loops. If the full massive LO cross section is multiplied by the K factor obtained in the heavy quark limit, a reliable approximation is obtained, within 10% for the top quark contribution to the production cross sections¹¹. Thus it will be sufficient to derive the QCD corrections to squark loops in the heavy squark limit. This can be done by extending the scalar low-energy theorems to squarks. We performed this calculation in the approximation of degenerate squark flavors and very heavy gluinos so that the latter decouple. The effective Lagrangian mediated by a squark loop reads¹⁰

$$\mathcal{L}_{eff} = \frac{\alpha_s}{48\pi} G^{a\mu\nu} G^a_{\mu\nu} \frac{H}{v} \left\{ 1 + \frac{25}{6} \frac{\alpha_s}{\pi} + \mathcal{O}(\alpha_s^2) \right\} \quad (11)$$

The amplitudes can be obtained from effective diagrams in analogy to Fig. 7. They were added to the massive quark amplitudes and contracted with the massive LO form factors in the virtual corrections. In this way we derived the most reliable approximation. The K factors differ only by less than $\sim 10\%$ from the K factors for the quark loops alone¹⁰. This is shown in Fig. 8, which presents the K factors with and without squark loops for a common squark mass of 200 GeV, for which the LO cross sections are significantly enhanced. Thus the full K factors can simply be approximated by the massive K factors to the quark loops alone, while the LO cross sections should include the massive squark contributions. This approximation is valid, because the QCD corrections for heavy particle loops are dominated by soft and collinear gluon effects.

2.3 Soft gluon resummation

The results of the last paragraph provide a strong motivation for the resummation of soft gluon effects in the Higgs boson production cross sections. This step has been carried out for a common squark mass $m_{\tilde{Q}} = 1$ TeV, so that squark loops can be neglected¹⁰. Moreover, we worked in the heavy quark limit, which provides an approximation to the cross sections within $\sim 25\%$ for $tg\beta \lesssim 5$. For larger values of $tg\beta$ the bottom contribution becomes significant. Finally the gq and $q\bar{q}$ initial states will be neglected, since their contribution only amounts to $\sim 10\%$ ⁹. Within this approximation the partonic cross sec-

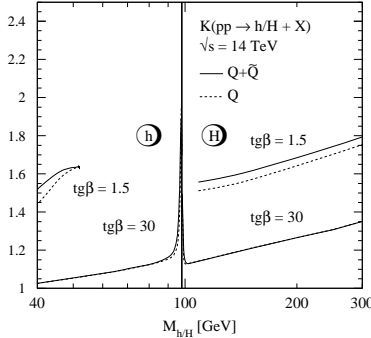


Figure 8: K factors of the cross sections $\sigma(pp \rightarrow h/H + X)$ with [solid lines] and without [dashed lines] squark loops as a function of the corresponding scalar Higgs mass for two values of $\text{tg}\beta = 1.5, 30$. The common squark mass has been chosen as $M_{\tilde{Q}} = 200$ GeV.

tions factorize into three pieces²⁰,

$$\hat{\sigma}_{gg} = \sigma_0^\phi \kappa_\phi \rho_\phi \quad (12)$$

The factors κ_ϕ are fixed by the effective Lagrangian at NNLO^{20,21}:

$$\begin{aligned} \kappa_A &= 1 & (13) \\ \kappa_{h,H} &= 1 + \frac{11}{2} \frac{\alpha_s(M_t)}{\pi} + \frac{3866 - 201 N_F}{144} \left(\frac{\alpha_s(M_t)}{\pi} \right)^2 \\ &\quad + \frac{153 - 19 N_F}{33 - 2 N_F} \frac{\alpha_s(M_H) - \alpha_s(M_t)}{\pi} + \mathcal{O}(\alpha_s^3) \end{aligned}$$

while the correction factors ρ_ϕ originate from effective diagrams. At LO they are normalized as $\rho_\phi = \delta(1 - z)$ with $z = M_\phi^2/\hat{s}$. It has been shown for the Drell–Yan process that for $z \lesssim 1$ the cross section factorizes into soft gluon contributions, jet functions containing collinear gluon effects and a hard matrix element²². From this factorization the Sudakov evolution equation can be derived²³:

$$M_\phi^2 \frac{\partial \rho_\phi}{\partial M_\phi^2} = W_\phi \otimes \rho_\phi \quad (14)$$

where the convolution is defined as $f \otimes g = \int_z^1 dz' f(z') g(z/z')$. The evolution kernel W_ϕ can be determined from the perturbative result by matching the leading terms with the perturbative expansion of the solution to Eq. 14. In this way we have determined the first term in the expansion of W_ϕ and thus resummed the soft gluon effects with NLO accuracy. The renormalization and mass factorization defined the strong coupling α_s and the parton densities in

the $\overline{\text{MS}}$ scheme. The resummed result has then been used as a generating functional for the perturbative expansion up to NNLO. The NLO terms of ρ_ϕ read as²⁰

$$\rho_{h,H}^{(1)} = 12\mathcal{D}_1(z) - 24\mathcal{E}_1(z) - 6\mathcal{D}_0(z)L_\mu + \pi^2\delta(1-z) \quad (15)$$

$$\rho_A^{(1)} = \rho_{h/H}^{(1)} + 6\delta(1-z) \quad (16)$$

where

$$\mathcal{D}_i(z) = \left[\frac{\log^i(1-z)}{1-z} \right]_+, \quad \mathcal{E}_i(z) = \log^i(1-z), \quad L_\mu = \log\left(\frac{\mu^2}{M_\phi^2}\right) \quad (17)$$

The term $\mathcal{E}_1(z)$ extends the conventional resummation techniques, which only resum the soft gluon logarithms $\mathcal{D}_i(z)$. The leading part of the $\mathcal{E}_i(z)$ terms is of a pure collinear nature and thus universal as well. The consistency of this extension has not been proved so far. However, it is important to note that these terms are large for LHC processes, and thus relevant. Moreover, the analogous analysis for the Drell–Yan process and deep inelastic scattering reproduced the leading terms in $\mathcal{E}_i(z)$ at the NNLO level so that we got confidence that they are universally factorizing in the collinear limit. The NNLO expansion of ρ_ϕ can be cast into the form²⁰

$$\begin{aligned} \rho^{(2)} &= 3 \left\{ 24\mathcal{D}_3(z) + (-2\beta_0 - 36L_\mu)\mathcal{D}_2(z) + (-24\zeta_2 + 2\beta_0L_\mu + 12L_\mu^2)\mathcal{D}_1(z) \right. \\ &\quad + (48\zeta_3 + 12\zeta_2L_\mu - \frac{1}{2}\beta_0L_\mu^2)\mathcal{D}_0(z) - 48\mathcal{E}_3(z) \\ &\quad + (4\beta_0 + 24 + 72L_\mu)\mathcal{E}_2(z) + (48\zeta_2 - 4\beta_0L_\mu - 24L_\mu - 24L_\mu^2)\mathcal{E}_1(z) \\ &\quad \left. + (18\zeta_2^2 - 36\zeta_4 - \frac{2909}{432}\beta_0 + \zeta_2\beta_0L_\mu - 24\zeta_3L_\mu - 6\zeta_2L_\mu^2)\delta(1-z) \right\} \\ \rho_A^{(2)} &= \rho_{h/H}^{(2)} + 3 \left\{ 24\mathcal{D}_1(z) - 12L_\mu\mathcal{D}_0(z) - 48\mathcal{E}_1(z) \right. \\ &\quad \left. + (12\zeta_2 + 6 + \beta_0L_\mu)\delta(1-z) \right\} \end{aligned} \quad (18)$$

with $\beta_0 = (33 - 2N_F)/6$. The analogous analysis of the Drell–Yan process results in a reliable approximation up to NNLO²⁰ so that the NNLO results of Eq. 18 are expected to be a reliable approximation of the NNLO corrections to the Higgs production cross sections. The correction factors convoluted with NLO parton densities are presented in Fig. 9 as a function of the corresponding Higgs mass. The NLO expansion of ρ_ϕ is denoted by γ_1 and the NNLO expansion by γ_2 . We observe a good agreement of γ_1 with the exact NLO result, within $\sim 5\%$, while the correction factor γ_2 turns out to be large²⁰. This,

however, is caused by the use of NLO quantities in all perturbative orders of the correction factor. A consistent analysis requires LO α_s and parton densities for the LO correction factor and NNLO quantities for γ_2 . This reduces the NLO correction factor to a level of ~ 1.5 , which is significantly smaller than the NLO and γ_1 curves in Fig. 9. Thus in order to obtain a NNLO prediction NNLO parton densities are needed, which, however, are not available so far. Therefore a consistent theoretical prediction of the NNLO Higgs production cross sections is not yet possible.

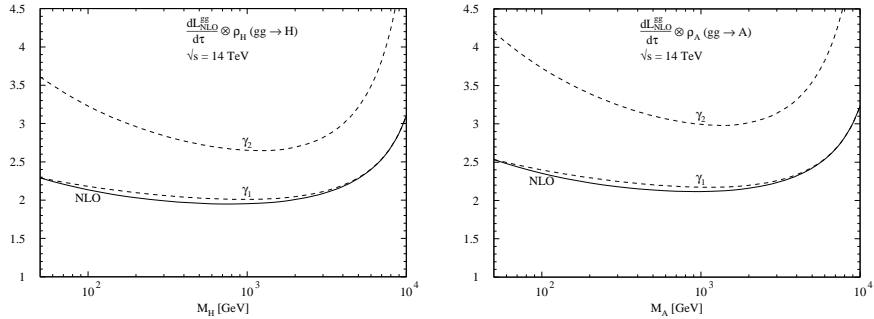


Figure 9: *Exact and approximate two- and three-loop correction factor convoluted with NLO gluon densities in the heavy top quark limit for the MSSM Higgs bosons. The CTEQ4M parton densities have been adopted with $\alpha_s(M_Z) = 0.116$ at NLO.*

3 Conclusions

We have reviewed the theoretical status of the production of neutral MSSM Higgs bosons at the LHC. The NLO QCD corrections are large and positive, while the theoretical uncertainty estimated from the residual scale dependence is reduced significantly. The squark loop contributions become sizeable for squark masses below ~ 400 GeV. The K factors, however, deviate by less than $\sim 10\%$ if squark loops are included. The K factors depend strongly on the MSSM parameter $\tan\beta$. Finally we have performed the soft gluon resummation for the Higgs production cross sections, which we expanded up to NNLO in order to get a reliable estimate of the NNLO corrections. These turn out to be potentially large. However, a consistent phenomenological analysis at NNLO requires NNLO parton densities, which are not yet available.

Acknowledgements

I would like to thank S. Dawson, A. Djouadi, D. Graudenz, M. Krämer, E. Laenen and P. Zerwas for the fruitful collaboration in the presented work.

References

1. S. Dimopoulos and H. Georgi, Nucl. Phys. **B193** (1981) 150; N. Sakai, Z. Phys. **C11** (1981) 153; K. Inoue et al., Prog. Theor. Phys. **67** (1982) 927; (E) **70** (1983) 330; **71** (1984) 413; E. Witten, Nucl. Phys. **B231** (1984) 419.
2. Y. Okada et al., Prog. Theor. Phys. **85** (1991) 1; H. Haber and R. Hempfling, Phys. Rev. Lett. **66** (1991) 1815; J. Ellis et al., Phys. Lett. **B257** (1991) 83; M. Carena et al., Phys. Lett. **B355** (1995) 209; H. Haber et al., Z. Phys. **C75** (1997) 539.
3. P. Janot, Proceedings, Europhysics Conference on High Energy Physics, Jerusalem 1997.
4. H. Georgi et al., Phys. Rev. Lett. **40** (1978) 692.
5. J. Gunion et al., Nucl. Phys. **B294** (1987) 621; S. Moretti and K. Odagiri, Phys. Rev. **D55** (1997) 5627.
6. E. Eichten et al., Rev. Mod. Phys. **56** (1984) 579.
7. A. Krause et al., preprint CERN-TH/97-137, hep-ph/9707430.
8. E. Richter-Was et al., preprint CERN-TH/96-111.
9. M. Spira et al., Nucl. Phys. **B453** (1995) 17 and references therein.
10. S. Dawson et al., Phys. Rev. Lett. **77** (1996) 16.
11. M. Spira, preprint CERN-TH/97-68.
12. G. 't Hooft and M. Veltman, Nucl. Phys. **B44** (1972) 189; P. Breitenlohner and D. Maison, Commun. Math. Phys. **52** (1977) 11.
13. S. Larin, Phys. Lett. **B303** (1993) 113.
14. J.G. Körner et al., Z. Phys. **C54** (1992) 503.
15. G. Altarelli and G. Parisi, Nucl. Phys. **B126** (1977) 298.
16. J. Ellis et al., Nucl. Phys. **B106** (1976) 292.
17. S.L. Adler, Phys. Rev. **177** (1969) 2426; J.S. Bell and R. Jackiw, Nuovo Cimento **60A** (1969) 47.
18. D. Sutherland, Nucl. Phys. **B2** (1967) 443; M. Veltman, Proc. Roy. Soc. **A301** (1967) 107.
19. S.L. Adler and W.A. Bardeen, Phys. Rev. **182** (1969) 1517; R. Jackiw, Lectures on Current Algebra and its Applications (Princeton University Press, 1972).
20. M. Krämer et al., preprint CERN-TH/96-231.
21. K.G. Chetyrkin et al., Phys. Rev. Lett. **79** (1997) 353.
22. J.C. Collins et al., in *Perturbative Quantum Chromodynamics*, ed. A.H. Mueller (World Scientific, Singapore, 1989).
23. H. Contopanagos et al., Nucl. Phys. **B484** (1997) 303.